Drug combination nanoparticles targeted to ICAM-1 on breast cancer cells enhance cellular drug exposure *in vitro* and in mouse model

Linxi Zhu

A thesis

submitted in partial fulfillment of the

requirements for the degree of

Master of Science

University of Washington

2021

Committee:

Rodney JY Ho

Edward Kelly

Program Authorized to Offer Degree:

Pharmaceutics

University of Washington

Abstract

Drug combination nanoparticles targeted to ICAM-1 on breast cancer cells enhance cellular drug exposure *in vitro* and in mouse model

Linxi Zhu

Chair of the Supervisory Committee:
Dr. Rodney JY Ho
Department of Pharmaceutics

Triple-negative breast cancer (TNBC) is a subtype of breast cancer that lacks the expression of 3 cell receptors--the estrogen receptor (ER), progesterone receptor (PR) and epidermal growth factor receptor-2 (Her2) --that cancer cells use for uncontrolled growth. A number of drugs that interfere with the aforementioned receptors are available to control breast cancer growth. However, cells that have lost these receptors are difficult to treat, and typically lead to aggressive metastatic cancer cell spread with progressive disease. Due to the lack of druggable cell-specific targets, there are limited therapeutic options, leading to higher metastasis rates and poor treatment outcomes. To address these limitations in breast cancer treatment, this thesis research leverages on a nanoparticle technology which has been previously proven to enable the assembly of potent drugs in combination to provide long-acting effects in the body. Specifically, this research assembled a highly potent two-drug combination of gemcitabine (G)

and paclitaxel (T) into drug combination nanoparticles or DcNP. We then determined whether a cell receptor that over-expressed in breast cancer cells, called Intercellular Adhesion Molecule 1 (ICAM-1), can be used to enhance uptake and localization of a highly potent, but non-selective gemcitabine and paclitaxel (GT) cancer drug combination assembled in a small nano-size particle. The two drugs—gemcitabine (G) and paclitaxel (T)—are currently used in clinic with some effectiveness, but exhibit dose-limiting toxicity. Our overarching goal is determining whether ICAM-1 targeted drug combination particles could provide higher drug potency and increase the margin of safety. We found that incorporating two anti-cancer drugs—gemcitabine (G) and paclitaxel (T)—into nanoparticles and targeting them to ICAM-1 overexpressed on breast cancer 4T1 cells enhanced drug uptake and retention in the cells and tumor laden tissues. Targeting to ICAM-1 is achieved by coating GT-DcNP with an ICAM binding peptide fragment sequence (ITDGEATDSG) derived from its endogenous binding ligand lymphocyte function-associated antigen 1 (LFA-1) [referred to as LFA1-P]. We found that coating LFA1-P on DcNP provides preferential localization of G and T to breast cancer cells 4T1 and MDA-MB231. This novel anti-cancer drug combination nanoparticle (GT-DcNP-LFA1-P) can enhance the effects of two parent anti-cancer drugs (in solution) and enable sustained drug concentrations in target cells both in vitro and in vivo.

In this thesis, the target selectivity of different ligand incorporated DcNPs was designed, prepared, characterized and finally evaluated in an MDA-MB-231 breast cancer cell line. ICAM-1 ligand (LFA1-P) showed the best target ability. We found that compared to a non-targeted GT-DcNP counterpart (when given a high dose to 4T1 metastatic breast cancer mice), incorporation of LAF1-P in DcNP targeted to ICAM-1 on breast cancer cells enhanced the accumulation of G and T in lung tissue by 2.2 and 1.7 fold ($P \leq 0.05$), respectively. In an aggressive 4T1 breast

metastatic tumor model, we found that inclusion of LFA1-P enhanced GT-DcNP mediated tumor inhibitory effects at a low single GT (5/0.5 mg/kg, IV) dose. While ICAM-1 targeted and non-targeted GT-DcNP exhibited significant tumor suppression compared to an untreated control, targeted LAF-1-P-GT-DcNP exhibited a higher degree of significance over that of free GT treated mice.

Collectively, based on the ICAM-1 overexpression on TNBC breast cancer GT-DcNP-LFA1-P, mimicking LFA-1, the ICAM-1 ligand was designed and verified to enable the targeting of GT in drug-combination particles to breast cancer cells leading to enhanced tumor tissue accumulation and suppression of 4T1 tumor growth in the lung. This approach may be applicable for developing other potent cancer chemotherapeutic combinations to provide targeted and synchronized drug combination delivery to advancing and metastatic cancer cells for increasing efficacy and safety.

TABLE OF CONTENTS

LIST OF TABLES

LIST OF FIGURES

ACKNOWLEDGEMENTS

I would like to first acknowledge my mentor, Professor Rodney JY Ho, for his guidance and support throughout my graduate school experience. His caring heart and rigorous practice of science has helped me grow both as a person and pharmaceutical scientist. I thank him from the bottom of my heart for providing me this opportunity and for everything he has taught me and done for me. The training I have received in the Ho laboratory encompasses a broad scope of science that I am truly grateful for having experienced. I also had the pleasure and good fortune to have Professor Edward Kelly in my committee to guide my thesis. I have really enjoyed getting to know Edward as both a faculty member and member of my committee and I would like to thank him for his support and advocacy for the graduate students at UW.

To Dr. Qingxin Mu, I would like to thank him for his guidance and consistent support. He is incredibly helpful and insightful. He has a wonderful way of teaching how to design experiments and how to ask questions. I've learned valuable lessons from him. Next, I want to thank all of Ho research team members and those involved in my project and give me help during these two years. Working with the team has been a unique experience, and I will value this experience throughout my life. I would also like to thank the staff and faculty of the pharmaceutics department, all of whom never stopped challenging me, and helping me develop my ideas.

Finally, I would like to thank my family and friends who supported me over the years. They all kept me going, and my thesis would not have been possible without them.

The research is supported in part by NIH grants UM1 AI 12176, R66 AI 149665, and University of Washington Royalty Research Fund (A154601).

1 INTRODUCTION

Breast cancer is the most common cancer in women worldwide and the second most common cancer overall[1]. Due to high histological grade, prone to distant metastasis, is a subtype of breast cancer with the worst prognosis and the highest mortality rate. Triple-negative breast cancer (TNBC) is a subtype of breast cancer that lacks the expression of 3 cell receptors--the estrogen receptor (ER), progesterone receptor (PR) and epidermal growth factor receptor-2 (Her2) that cancer cells used for uncontrol growth. A number of drugs which interfere with the aforementioned are available to control breast cancer growth. However, cells that lost these receptors are difficult to treat, and typically lead to aggressive metastatic cancer cell spread with progressive disease. Due to the lack of druggable cell-specific targets, there is limited therapeutic options, leading to higher metastasis rates and poor prognosis. TNBC is a basal-like breast cancer, accounts for approximately 15-20% of all breast cancers and is biologically more aggressive, and have shorter progression-free survival and overall survival relative to non-TNBC breast cancer patients[2]. TNBC is basically unresponsive to drugs intended to interfere with endocrine dependent cancer growth, therefore these patients mainly rely on non-specific and cytotoxic chemotherapy[3], Its poor prognosis and high mortality still cannot be further improved[4]. To date, there are a variety of treatment for triple negative breast cancer, including immunotherapy medicines such as programmed death-ligand 1(PDL1) inhibitors, DNA damaging agents such as poly ADP ribose polymerase (PARP) inhibitors, targeted epidermal growth factor receptor (EGFR) and vascular endothelial growth factor (VEGF) inhibitors. However, these methods still have reflected poor response, high toxicity and develops multidrug resistance and, to date, no clinical trial has been successful. Therefore, finding effective and safe

treatments for triple-negative breast cancer is urgently needed to make clinical impact for patients with TNBC, including those who progress to metastatic breast cancer.

With the development and advances in nanotechnologies, many researchers have been developing new strategies to leverage nano-mediated targeted drug delivery systems for the treatment of breast cancers. While TNBC lack druggable receptor target to direct nanoparticles carrying drug to cells, there are other cancer cell receptors which can be exploited to enhance cancer cell selectivity for localization of drugs loaded in nanoparticles. Using molecular biological targets on the surface of TNBC cells, such as epidermal growth factor (EGF), transferrin, etc. target specific tumor sites through ligands, side effects can be reduced, and efficacy can be improved[5].

Lymphatic vessels are a primary route for metastasis of many kinds of cancers including breast, liver, pancreas and head and neck cancers. The microenvironment in the lymph, lymph vessels and lymph nodes, including chemokines and lymph angiogenesis, can mediate the metastatic spread from the sentinel lymph nodes to periphery and beyond (disseminated spread of cancer)[6]. In addition, lymph angiogenesis within the sentinel lymph nodes is also associated with tumor metastasis to distant sites[7]. Lymph node metastasis is an important prognostic factor of breast cancer and its elimination is imperative to control cancer progression. Currently, most therapeutics monitoring focuses on plasma drug concentration, which may not accurately reflect lymphatic drug exposure.

Recently, our laboratory has developed a targeted, long-acting and drug combination nanoparticle composition and process, referred to as DcNP platform technology. The excipient and process provide a way to assembled multiple drug combinations in nanoparticles as a pharmaceutical drug combination product. This technology enables formulation of a combination

of three or more HIV drugs in a lipid-stabilized single nanosuspension[8]. When a set of drug-combinations for HIV are formulated in DcNP and administered in non-human primates, drug formulated in DcNP platform is verified to produce long-acting and enhanced HIV host lymphocyte drug exposure in non-human primates; thus, a number of drug combinations are currently under development intended for treatment of HIV/AIDS as a long-acting and targeted therapy. The concentrations of orally administered HIV drugs (including current fixed-dose combination tablets) in lymph nodes are often lower than that found in blood and plasma, and thus are not sufficient for effective treatment to clear residual virus in lymph tissues[9–11]. In contrast, the long-acting injectable 3-HIV-drug in DcNP nanoformulation derived from this technology can achieve sustained drug levels in both plasma and lymph node mononuclear cells in non-human primates for 2 weeks or more[8,12]. The combination of drugs with diverse mechanisms in one formulation can also reduce drug resistance[8]. Moreover, the combined formulation could also improve patient compliance. The lymphatic targeting and long-acting features of the injectable DcNP provide a great opportunity for therapy of metastatic cancers. Therefore, we applied the targeting and long-acting platform to cancer treatment by combining GT into DcNP, increased the systemic circulation time of gemcitabine and enhanced the pharmacokinetics of the two drugs[13,14]. This nanoparticle mediated delivery system improved benefits of drug combination therapy, achieved passive targeting of cancer, reduced toxicity. However, as TNBC lacks druggable specific ligands or receptors, DcNP cannot actively target TNBC cells with well-described markers express on the cancer cells. In order to further minimize off-target effects, enables TNBC-specific delivery and achieve superior therapeutic, we selected a molecule highly expressed in TNBC cells as a target, and further optimized the GT DcNP formulation by adding a ligand to enable target selectivity of GT delivery to cancer cells.

The incorporation of targeting ligands to DcNP can facilitate active targeting of DcNP to receptors present on target cells, thereby enhancing cell internalization and/or specific uptake through receptor-mediated endocytosis compared with free drugs or passively targeted nanosystems[15,16]. Active targeting is essential for delivering drugs to the target site while avoiding normal tissues, thereby enhancing the therapeutic efficacy, and limiting side effects.

It was recently reported that TNBC cell lines express on surface a molecule intercellular adhesion molecule-1 (ICAM-1, also known as CD54 transmembrane protein) and cell matrix protein integrin[17,18]. ICAM-1 is a transmembrane glycoprotein protein (MW ~85-110 kD). LFA-1 has been reported as the ligand that binds to ICAM-1[19–21]. ICAM-1 has low expression on the membranes of leukocytes and endothelial cells. The cell surface ICAM-1, which binds to LFA-1 of the integrin, part of the endothelial cell matrices within the vasculature, plays an important role in tumor metastasis, spread and disease progression. Thus, expression of ICAM-1 may be involved in the regulation of tumor susceptibility of defensive cells. Therefore, ICAM-1, overexpressed in cancer cells may serve as a molecular target and biomarker for TNBC in the development of cell-specific drug therapy.

A peptide sequence, ITDGEATDSGC (referred to as LFA1-P peptide), derived from the I-domain of the αL-subunit of LFA-1 integrin, inhibits LFA-1 and ICAM-1 interaction by binding to ICAM-1 (and also prevent ICAM-1 mediated receptor internalization)[19–21]. The LFA1-P peptide displayed receptor-mediated endocytosis, indicating its possible use as a targeting moiety for intracellular drug delivery. Indeed, it has been shown that LFA1-P conjugated nanoparticles can target to ICAM-1 and further alter cell response[22].

Integrin alphaV beta3 (αvβ3), an extracellular matrix receptor, has been identified to play a direct role in tumor cell growth, invasion, metastasis, and angiogenesis[23]. High expression of

αvβ3 has been identified in a number of tumor types including breast cancer. Arginine–glycine–aspartic acid (Arg-Gly-Asp, RGD) peptides are targeting ligands that specifically bind to integrin αvβ3. RGD peptide has been shown to block glioma cell growth *in vitro*[24,25] and also inhibit bone metastasis induced by MDA-MB-231 breast cancer cells in rats[24,26]. Therefore, RGD is also a potential targeting ligand in triple negative breast cancer.

In this study, we aim to utilize this DcNP platform on triple negative metastatic breast cancer target treatment and evaluate whether the incorporation of a peptide mimicking ICAM-1 ligand binding domain can improve the selectivity of drugs in DcNP and mitigate tumor growth *in vivo* and *in vitro*. We selected 4T1 metastatic and aggressive breast cancer cell line as TNBC cells model, evaluated the expression of ICAM-1 on the surface of 4T1 cells by immunofluorescence, verified the binding and uptake ability of cells to ICAM-1 ligand, LFA1-P peptide incorporated DcNP (DcNP-LFA1-P). With data validating time and concentration dependent DcNP, DcNP-LFA1-P and GT free drug combination uptake in 4T1 model, additional human breast cancer cells, including MDA-MB-231, SKBR3 with varying ICAM-1 expression. With a lead candidate DcNP-LFA1-P containing GT combination, ICAM-1 targeted effect of DcNP was evaluated in 4T1 mouse breast cancer model.

2 METHODS

2.1 Comparison and evaluation of different nanoparticle preparation methods

2.1.1 Materials

Gemcitabine free base (>99%; 2',2'-Difluorodeoxycytidine; CAS 95058-81-4) and paclitaxel (>99.5%; CAS 33069-62-4) were purchased from LC Laboratories (Woburn, Massachusetts). 1,2-distearoyl-sn-glycero-3-phosphocholine (DSPC) and 1,2-distearoyl-sn-glycero-3-phosphoethanolamine-N- [amino (polyethylene glycol)-2000] (ammonium salt) (DSPE-PEG_{2000}) (GMP grade) were purchased from Cordon Pharma (Liestal, Switzerland). Indocyanine green (ICG; $C_{43}H_{47}N_2NaO_6S_2$; sodium 2-[7-[3,3-dimethyl-1-(4-sulfonatobutyl) benz[e]indolin-2-ylidene] hepta-1,3,5-trien-1-yl]-3,3-dimethyl-1-(4-sulfonatobutyl) benz) was purchased from TCL America. Anhydrous ethanol was purchased from Decon Pharmaceuticals (King of Prussia, PA). All other reagents used were of analytical grade or higher.

2.1.2 Formulation and characterization of DcNP

2.1.2.1 Preparation of gemcitabine and paclitaxel in drug combination nanoparticles

Drug combination nanoparticles or DcNP containing gemcitabine (G) and paclitaxel (T) were prepared by first dissolving GT and lipid excipients-DSPC and DSPE-PEG_{2000} in ethanol-chloroform and buffer, followed by controlled solvent removal using a rotor evaporator to form thin film coated on glass surface; this is followed by hydration to form GT-DcNP in suspension. The large GT-DcNP suspension particle size is reduced by sonication and other methods as discussed below.

Briefly, to prepare GT-DcNP, G, T, DSPC and DSPE were dissolved in the mixture of chloroform, ethanol, and deionized water at 60°C. Solvent was removed by rotary evaporation to

form a thin film, which was vacuum desiccated to remove residual solvent. The thin film was rehydrated with PBS at 60°C for 2 hours. The heterogenous and large DcNP particulate matters in the hydrated initial suspension was reduced by four different size reduction methods. Particle size of DcNP product was determined by photon correlation spectroscopy using a NICOMP 380 ZLS (Particle Sizing Systems, Santa Barbara, CA). Drug association efficiency (AE%) was determined by dialyzing 100 μL of the DcNP suspension (6-8k MWCO) against 1000 x volume (100 mL, pH=7.4) of bicarbonate buffered saline for 4 hours at room temperature. Drugs were extracted by acetonitrile and the resultant drug concentrations were measured by a Shimadzu HPLC-UV system (Kyoto, Japan). Drug concentration were determined for both pre- and post-dialysis of DcNP suspensions to determine the degree of drug association to DcNP as the dialysis membrane with 6-8k MWCO only permit removal of drug not associated with DcNP (which are much larger than molecular weight of 8k). The in-depth characterization of the final GT DcNP product is presented in 2.5.2 and 2.5.3.

2.1.2.2 Size reduction of DcNP in suspension

The rehydrated GT-DcNP or control DcNP without drug are subjected to various size-reduction process as described below. The initial GT-DcNP in suspension are allowed to hydrate at 60ºC for approximately 2 hr and subjected to following size reduction methods.

2.1.2.3 Size reduction with a probe sonicator

The solution was sonicated by a tip sonicator for 3 min.

2.1.2.4 Extrusion with a LIPEX extruder

After assembling the thermo-barrel extruder according to operation manual (100nm polycarbonate membrane, Fig. 1), the thermo-barrel jacket was heated to ~ 67-70 °C by a

circulating water bath. Deionized water was used to flush and wet the nucleopore membrane with 50nm pore size. The delivery pressure was set to between 600 and 700 psi under nitrogen gas. After the first extrusion pass was complete, the extruder was refilled with the freshly extruded suspension and the extrusion process was repeated for 10 times to obtain homogenous suspension of DcNP.

2.1.2.5 Extrusion with an Avanti mini-extruder

After assembling the mini-extruder with a 100 nm polycarbonate filter (Fig. 2), the extruder stand with heating block was placed onto a hot plate. A thermometer was inserted into the well provided in the heating block. The temperature of the heating block was allowed to reach ~67-70 °C, and then Deionized water was loaded into one side of the gas-tight syringes and carefully placed into one end of the mini-extruder. The empty gas-tight syringe was inserted into the other end of the mini-extruder, gently pushed the plunger of the filled syringe to wet the membrane. Sample was completely transferred to the alternate syringe and followed by operation above for 30 times.

2.2 ICAM-1 expression in human and non-human primate TNBC cells

2.2.1 Materials and cell lines

Goat anti-mouse ICAM-1 Polyclonal antibody (cat. no. 16174-1-AP) was purchased from Proteintech Group (Rosemont, IL). The HA58 mAb (mouse anti-human ICAM-1) was from BioeLgend, San Diego, CA. Goat anti-mouse IgG (Alexa Fluor® 555; Cat. No. 405324) Antibody was purchased from BioeLgend, San Diego, CA. Goat anti-rabbit IgG H&L (Alexa Fluor® 555; cat. no. ab150078) were purchased from Abcam. Frozen 4T1 cells, MDA-MB-231 cells, L929 cells and SKBR3 cells were purchased from ATCC.

2.2.2 Immunofluorescence analysis of ICAM expression on cells

ICAM-1 expression in 4T1, MDA-MB-231, SKBR3 and L929 cells was detected by immunofluorescence using ICAM-1 specific antibody. 30,000 cells/well were seeded into sterilized 8-well chamber slide. After overnight incubation, the cells were fixed for 10 min in 4% (w/v) paraformaldehyde/PBS at room temperature. Blocking solution (5% BSA/PBS) was added and incubated 1 hour at room temperature. After washing by PBS (3 times, 3 min/washing), anti-ICAM-1 antibody (diluted in 1% BSA/PBS) was then added to the wells. After 1.5 h room temperature incubation, primary antibody was removed, Alexa 555-conjµgated secondary antibody (diluted in 1% BSA/PBS) was then added and incubated for 1 hour at room temperature. Cells were then washed by PBS (3 times, 3 min/washing), chamber wall was removed, and mounting medium was added onto the slide. ICAM-1 expression on cells was detected with a fluorescence microscope.

2.3 Evaluation and selection of potential target ligands for TNBC cell

2.3.1 ligand incorporated drug free nanoparticle (NP) ICG Preparation

Ligand incorporated NP ICG were prepared by thin film hydration and sonication. Briefly, lipid excipients and ligands were dissolved in the mixture of chloroform, ethanol, and deionized water (10: 10: 1 v/v) at 60°C. Solvent was removed by rotary evaporation to form a thin film, which was vacuum desiccated to remove residual solvent. The thin film was rehydrated with PBS at 60°C for 2 hours. The NP diameter was reduced to~50 nm with 15 minutes of water bath sonication at ~45°C. For NP-ICG, ICG dissolved in ethanol was added to the lipid mixture before rotary evaporation. The particle size of NP and NP-ICG were determined by a NICOMP 380 ZLS (Particle Sizing Systems, Santa Barbara, CA). The preparation was performed under dark conditions and light exposure was avoided. Detailed formulations were showed in Table1.

2.3.2 ICG fluorescence quantification

To quantify ICG concentration the near IR Fluorescence measurements were performed on a Victor3 V 1420-040 Multilabel Plate Reader (Perkin Elmer; Waltham, MA) with a tungsten-halogen continuous wave lamp (75 w, spectral range 320-800 nm) and excitation (769 ± 41 nm) and emission (832 ± 37 nm) filters (Semrock; Rochester, NY) using 100 µL of sample in flat bottom, untreated 96-well plates.

2.3.3 Cell binding and uptake of ligand incorporated into nanoparticles or DcNP

2.3.3.1 Cell culture

MDA-MB-231 human breast cancer cells were purchased from American Type Culture Collection (ATCC) and grown in Dulbecco's Modified Eagle's Medium (DMEM) supplemented with 10% fetal bovine serum and 1% antibiotics. Cells were cultured in an incubator maintained at 37°C and 5% CO2 with 95% humidity.

2.3.3.2 Dose response of cell surface binding of ICG tagged nanoparticles

The experimental conditions were similar to section 2.2.3.2. Briefly, cells were seeded on a 6-well plate (600,000/well). After overnight incubation, ICG tagged nanoparticles (NP) in different (total lipid excipient) concentrations (6 mM, 4 mM, 2 mM, 1 mM, 0.5 mM, 0 mM) were added into wells (2 wells per concentration), and the plates were incubated at 4 °C for 1 hour. Cells were washed 3 times by 2 mL cold PBS (4 °C) after removing media in wells, then cells were dissolved in 200 µL solvent (5%PBS+95%DMSO). The resulting mixture was transferred into a 96-well microplate (black wall and clear bottom) for NIR fluorescence reading.

2.3.3.3 Evaluation of cyclic- and linear-LFA1-P ligands in their ability to mediate selective binding of ICG-NP to cancer cells

The effects of targeting peptide mediate ICG-NP uptake were evaluated in MDA-MB-231 cell. The indocyanine green (0.4 mole %) is added to NP to allow estimation of cell NP uptake by following near-infrared (NIR) fluorescence of ICG tagged on NP. Cells were seeded on a 6-well plate (~600,000/well) and allowed to grow overnight. Ligand-free ICG-NPs, ICG-NPs-linear-LFA1-P and ICG-NPs-cyclic- LFA1-P of different concentrations (2 mM, 1 mM, 0.5 mM, and 0 mM) were added into wells (1 well per concentration), and the plates were incubated at 4 °C for 1 hour. Plate was precooled before addition of ICG-NP. Cells were then washed 3 times by 2 mL cold PBS (4 °C) after draining media from wells by a vacuum pump, then dissolved in 200 μL solvent (5% PBS+95% DMSO). The resulting mixture was transferred into a 96-well microplate (black wall and clear bottom) for NIR fluorescence intensity measurement with a plate reader (Perkin Elmer Victor3).

2.3.3.4 Effects of ICG fraction on ability to trace NP in vitro and in vivo

Cells were seeded on 12-well plate (300,000/well). After overnight incubation, NP with 0.4% and 1% ICG contents with different lipid concentrations (2 mM, 1 mM, 0.5 mM, 0 mM) were added into wells (2 wells per concentration), and the plates were incubated at 4 °C for 1 hour and 37 °C for 20min, respectively. Cells were washed 3 times with 500 μL cold PBS (4 °C) after removing media in wells, then cells were dissolved into 100 μL solvent (100% DMSO). The resulting mixture was transferred into 96-well microplate (black wall and clear bottom) for NIR fluorescence reading.

2.3.3.5 Comparison of RGD and linear-LFA1-P incorporated NP (NP-LFA1-P) on the ability to enhance targeting of DcNP to cancer cells

Cells were seeded on 12-well plate (300,000/well). After overnight incubation, NP with RGD or linear-LFA1-P ligands and 1% ICG with different lipid concentrations (2 mM, 1 mM,

0.5 mM, 0 mM) were added into wells (2 wells per concentration), and the plates were incubated at 4 °C for 1 hour. Cells were washed 3 times with 500 μL cold PBS (4 °C) after removing media in wells, then cells were dissolved into 100 μL solvent (100% DMSO). The resulting mixture was transferred into 96-well microplate (black wall and clear bottom) for NIR fluorescence reading.

2.4 Evaluation of the influence of LFA1-P's density on the cell binding and uptake of NP

2.4.1 ICG-NP and LFA1-P incorporated ICG -NP Preparation

Ligand incorporated lipid-nanoparticle ICG were prepared by thin film hydration and sonication. Briefly, Lipid excipients and ICG were dissolved in the mixture of ethanol at 60°C, LFA1-P was firstly dissolved in 0.5 mg/mL mixture of chloroform/ethanol/methanol/water (20/15/3/4) and was added into lipid mixture before rotary evaporation. Solvent was removed by rotary evaporation to form a thin film, which was vacuum desiccated to remove residual solvent. The thin film was rehydrated in 0.45% NaCl with 20 mM NaHCO3 buffer at 60°C for 2 h. The NP diameter was reduced to ~50 nm with 15 minutes of water bath sonication at ~45°C. The particle size of IC- NP were determined by a NICOMP 380 ZLS (Particle Sizing Systems, Santa Barbara, CA). The preparation was performed under dark conditions and light exposure was avoided. Detailed formulations were showed in Table 1.

2.4.2 Analysis of ICG Fluorescence

For ICG-NP fluorescence measurements were performed on a Victor3 V 1420-040 Multilabel Plate Reader (Perkin Elmer; Waltham, MA) with a tungsten-halogen continuous wave lamp (75 w, spectral range 320-800 nm) and excitation (769 ± 41 nm) and emission (832 ± 37 nm) filters (Semrock; Rochester, NY) using 100 μL of sample in flat bottom, untreated 96-well plates.

2.4.3 Effects of LFA1-P density in enhancing 4T1 cells' binding to and uptake of DcNP using ICG-tagged nanoparticles

The cell binding and uptake was evaluated in 4T1 cell line by loading NP-LFA1-P into incubation medium and detected by near-infrared (NIR) fluorescence of ICG-NP. Cells were seeded on a 12-well plate (~300,000/well) and allowed to grow overnight. Ligand-free NP, NP with 0.5%, 1%, 2% and 5% LFA1-P of 0.5 mM (lipid concentration) were added into wells, and the plates were incubated at 4 ℃ (binding) for 1 hour or 37 °C (uptake) for 30 min. In binding study, plate was precooled for 10 minutes before addition of NP. Cells were then washed 3 times by 1 mL cold PBS (4 ℃) after draining media from wells by pipette, then dissolved in 200 μL DMSO. 180 μL resulting mixture was transferred into a 96-well microplate for NIR fluorescence of ICG in NP's intensity measurement with a plate reader as described above.

2.5 Evaluation of Cytotoxicity of DcNP, DcNP-LFA1-P and GT free drugs combination in 4T1 cells

2.5.1 Cell culture

Frozen 4T1 cells, MDA-MB-231 cells, L929 cells and SKBR3 cells were stored in the liquid nitrogen tank in Rodney J. Y. Ho's lab. DMEM and RPMI1640 supplemented with 10% fetal bovine serum and 1% antibiotics. Cells were cultured in an incubator maintained at 37°C and 5% CO2 with 95% humidity.

2.5.2 Formulation and characterization of DcNP

Ligand incorporated NP ICG were prepared by thin film hydration and sonication. Briefly, lipid excipients and ICG were dissolved in the mixture of ethanol at 60 C, LFA1-P was firstly dissolved in 0.5 mg/mL mixture of chloroform/ethanol/methanol/water (20/15/3/4) and was added into lipid mixture before rotary evaporation. Solvent was removed by rotary evaporation

to form a thin film, which was vacuum desiccated to remove residual solvent. The thin film was rehydrated in 0.45% NaCl with 20 mM NaHCO3 buffer at 60 °C for 2 h. The NP diameter was reduced to ~50 nm with 15 minutes of water bath sonication at~ 45 °C. The particle size of NP-ICG were determined by a NICOMP 380 ZLS (Particle Sizing Systems, Santa Barbara, CA).

2.5.3 Drug content determination by high performance liquid chromatography (HPLC)

2.5.3.1 Preparation of standards

T and G stock solutions (1 mg/mL in ethanol) were diluted to 100 μg/mL, 50 μg/mL, 20 μg/mL, 10 μg/mL, 5 μg/mL and 500 μg/mL, 200 μg/mL, 100 μg/mL, 50 μg/mL, and 25 μg/mL solutions with acetonitrile, respectively.

2.5.3.2 Extraction of bound drugs from DcNP

The bound drug can be quantified by dialysis experiments followed by HPLC quantification. Briefly, 100 μL of the DcNP suspension (6-8k MWCO) against 1000 x volume (100 mL, pH=7.4) of bicarbonate buffered saline for 4 hours at room temperature. Solution in the dialysis bags was collected.

2.5.3.3 Extraction of bound drug and total drug in DcNP

DcNP samples before and after dialysis were extracted by acetonitrile (100× dilution). After dilution, samples were briefly sonicated to get homogenous suspension and then centrifuged for 5 min at 10,000 g. Supernatant was collected for HPLC analysis.

2.5.3.4 HPLC

Supernatant was measured with a Shimadzu HPLC-UV system (Kyoto, Japan). Chromatographic separation was achieved using a Kinetex C18 column (100 Å, 5 μm, 4.6 mm × 100 mm) (Phenomenex, Torrance, CA). The flow rate was set to 1.0 mL/min with a 10 μl sample

injection volume. The mobile phase for separation consisted of pump A (Acetonitrile) and B (10 mM Ammonium Acetate in water). The gradient program used was as follows: pump B was set to 40% and increased to 100% over 5 minutes. The wavelength for detection of gemcitabine and paclitaxel was 254 nm.

The degree of drug association to DcNP or association efficiency was calculated as follow:

$$\text{Association efficiency}(AE\%) = \frac{(W_{total} - W_{free})}{W_{total}} \times 100\%$$

where W_{total} is the total weight of drug, W_{free} is the weight of un-associated free drugs.

2.5.4 Cytotoxicity assay

4T1 cells were seeded into duplicate wells of a 96-well plate (500 cells/well) at standard culture conditions of 5% CO_2 in air at 37°C. After an overnight incubation, DcNP- LFA1-P, DcNP and GT free drug combination (GT free drugs) were added into culture media at a final concentration of 0.128, 0.064, 0.032, 0.016, 0.008, 0.004, 0.002, 0.001, 0.0005, 0.00005 μg/mL and the plate were returned to the incubator. After another 3 days of culture, Alamar Blue was added directly into culture media at a final concentration of 10% and fluorescence intensity was measured after 1.5 hours incubation.

2.6 *Evaluation of LFA1-P mediated DcNP targeting to ICAM-1 expressed cancer cells In vivo using metastatic breast cancer model in mice*

2.6.1 Preparation of GT Cremophor EL (GT CrEL) drug combination

Paclitaxel was dissolved in ethanol (20 mg/mL) and diluted with an equal volume of Cremophor EL (Sigma-Aldrich, St. Louis, MO). The solution was then diluted 10× with a premade PBS solution of gemcitabine (hydrochloride salt) (12.65 mg/mL). Final concentrations

of drugs were 10/1 mg/mL GT CrEL drug suspensions were used within the same day of preparation due to instability.

2.6.2 In vivo GT-DcNP targeting and tumor inhibition study

All animal studies were conducted in accordance with University of Washington Institute of Animal Care and Use Committee (IACUC) approved protocols (protocol number 2372–06). The UW IACUC has specifically approved this study. Isoflurane was used for anesthesia during live animal imaging. 5–6 week-old female BALB/c mice were purchased from The Jackson Laboratory (Bar Harbor, Maine) and housed in an animal research facility for at least one week before use.

2.6.2.1 4T1 cell inoculation

Six-week-old, female BALB/c mice were used in this study. 4T1 cells were transfected with luciferase and green fluorescence protein (GFP) (4T1-luc); thus, 4T1 growth could be monitored based on that bioluminescence. 4T1-luc (2×10^5 cells) suspended in a 100 μL ice-cold HBSS suspension was intravenously inoculated through mouse tail veins. Mice were monitored for a two-week period. Bioluminescence of 4T1-luc from living mice was examined by a XENOGEN IVIS 200 imaging system (PerkinElmer, Inc. Waltham, MA). Mice received 150 mg/kg D-luciferin through intraperitoneal injections 10~15 min before imaging. The bioluminescence imaging parameters for living mice were set as follows: field of view, 12; excitation filter, closed; emission filter, open; exposure time, 120 sec; binning factor, 4; f/stop, 2. Total 4T1-luc bioluminescence emission from living mice was integrated using Live Image software (PerkinElmer, Waltham, MA).

2.6.2.2 Tumor progression in 4T1 metastatic breast cancer mice

Six-week-old, female BALB/c mice were inoculated with 2×10^5 4T1-luc cells IV in 100 µL HBSS on day 0. On day 1, 3, 5, 7, 10, 12, mice were euthanized immediately after live imaging and lungs were collected to quantify nodules amount under digital microscope (Fisher Scientific). The images were acquired by a Xenogen IVIS-200. The bioluminescence imaging parameters for living mice were set as follows: field of view, 24; excitation filter, closed; emission filter, open; exposure time, 180 sec; binning factor, 4; f/stop, 2. Bioluminescence intensity from living mice was integrated using Live Image software. Mouse lung tissue was fixed in formalin and stored in 70% EtOH.

2.6.2.3 Target effects of DcNP, GT CrEL drug combinations and DcNP-LFA1-P on metastatic breast cancer mice

Six-week-old, female BALB/c mice were inoculated with 2×10^5 4T1-luc cells IV in 100 µL HBSS on day 0. Three hours later, mice were given a single administration of saline, a CrEL drug combination, DcNP or GT DcNP-LFA1-P through IV injections (n = 8-15). The GT doses were 50/5 mg/kg for CrEL and DcNP formulations. On day 14, mice were euthanized immediately after live imaging and lungs were collected and placed in 12-well plates to quantify luminescence images. The images were acquired by a Xenogen IVIS-200. The bioluminescence imaging parameters for living mice were set as follows: field of view, 24; excitation filter, closed; emission filter, open; exposure time, 180 sec; binning factor, 4; f/stop, 2. Ex-vivo imaging parameters for lungs were set as follows: field of view, 10; excitation filter, closed; emission filter, open; exposure time, 30 sec; binning factor, 4; f/stop, 2. Bioluminescence intensity from living mice and lungs was integrated using Live Image software. Mouse lung tissue was fixed in formalin and stored in 70% EtOH.

2.6.2.4 Tumor inhibition effects of DcNP, CrEL drug combinations and DcNP-LFA1-P on metastatic breast cancer mice

Six-week-old, female BALB/c mice were inoculated with 2×10^5 4T1-luc cells IV in 100 μL HBSS on day 0. Three hours later, mice were given a single administration of saline, a CrEL drug combination, GT DcNP or GT DcNP-LFA1-P through IV injections (n = 5). The GT doses were 5/0.5 mg/kg for CrEL and DcNP formulations. On day 14, mice were euthanized, and lungs were collected Mouse lung tissue was fixed in formalin and stored in 70% EtOH.

2.6.3 Drug extraction and analysis

A liquid-liquid extraction was used to extract drugs from plasma or tissue homogenates. 50 μL of sample were transferred into 1.5 mL tubes with or without dilution by blank matrix to an appropriate concentration range. Samples were spiked by internal standards followed by the addition of acetonitrile. followed by the addition of 9 volumes of acetonitrile (450 μL). Samples were then vortexed and centrifuged at 4°C for 15 minutes at 14000 rpm. The supernatant was then removed and dried under nitrogen at 40°C. The dried samples were reconstituted in 20% methanol and 80% water in 50 μL.

2.6.4 Quantification of drugs by LC-MS/MS

Drugs were quantified by a Shimadzu HPLC system coupled to a 3200 QTRAP mass spectrometer (Applied Biosystems, Grand Island, NY). The HPLC system consisted of two Shimadzu LC-20A pumps, a DGU-20A5 degasser, and a Shimadzu SIL-20AC HT autosampler. The mass spectrometer was equipped with an electrospray ionization (ESI) TurboIonSpray source. The system was operated with Analyst software, version 1.5.2 (ABSciex, Framingham, MA).

Chromatographic separation of drugs was achieved using a Synergi column (100 × 2.0 mm; 4- μm particle size) with an inline C8 guard column (4.0 × 2.0 mm) (Phenomenex, Torrance, CA). An ammonium acetate buffer/reagent alcohol gradient was used to separate components. Analytes were monitored using multiple-reaction monitoring for positive ions. The following ion transitions were monitored: gemcitabine, m/z 264.066→112.000; paclitaxel, m/z 854.266→286.200; a stable labeled isotope (C813CH12ClF2N15N2O4) (m/z 267.067→115.100) was used as an internal standard for gemcitabine; docetaxel (m/z 830.312→549.3) was used as an internal standard for paclitaxel.

2.6.5 Statistical Analysis

Targeting and inhibition data were presented as the arithmetic mean ± standard error of the mean (SEM). The number of mice in all groups ranges from 3 to 5. Statistical analysis was performed using GraphPad Prism 7.04 (GraphPad Software Inc., San Diego, CA). Statistical comparisons were performed using students' t-tests were, two-way ANOVA was used to determine statistical significance for multiple treatment groups across studies. A P-value of ≤ 0.05 was considered statistically significant.

3 RESULTS AND DISCUSSIONS

3.1 Design and characterization of gemcitabine and paclitaxel drug combination nanoparticles with respect to process, particle size and degree of drug association to DcNP

As described in Materials and Methods, the gemcitabine (G) and paclitaxel (T) referred to as GT-drug-combination and lipid excipient mixtures were first hydrated into suspension, followed by particle size reduction by subjecting the suspension to ultrasonic energy input or sonication. Sonication is a traditional method, which has been shown to be capable of reducing particle size without the drug loss in preparing nanodrug combination in suspension. However, the size heterogeneity of DcNP drug particles necessitated investigating another approach. Thus, we evaluated extruding the particles in suspension through filters with defined pore size mounted in pressurized extruders to arrive to a final particle size below 200 nm in diameter. Two device, LIPEX extruder and Avanti mini-extruder, has been reported to make uniform populations of lipid and other polymeric nanoparticles by through filter-extrusion in an efficient manner. They are more appropriate methods for the preparation of laboratory-scale uniform size for final nanoparticles in suspension. Because T is a hydrophobic compound which forms aggregation complex with lipids, we found a disproportional and significant loss of T, not G after passage of the GT-DcNP through LIPEX extruder and Avanti mini-extruder (Table 2). Thus, extrusion through filter is not an appropriate method; and therefore, we used sonication as a chosen DcNP size reduction method with better control processes to prepare GT-DcNP for the data presented in Table2.

3.2 Evaluation of ICAM-1 expression on human and non-human primate TNBC cells

To investigate whether breast cancer cells express ICAM-1, which will be used for targeting drug combination in DcNP, we evaluated a LFA1-P peptide mimic of ICAM-1 ligand, LAF-1 peptide, which has been reported to optimally and selectively bind to ICAM-1[19–21]. To do so, we first used ICAM-1 selective antibody and verified cell expression by immunofluorescence staining, which is presented in Figure 3. The breast cancer cells of mouse 4T1 cells (A, C), human MDA-MB-231 cells (D) and SKBR3 cells (E) were tested. Among the three cell types tested, only the mouse 4T1 and human MDA-MB-231 breast cancer cells exhibited significant ICAM-1 cell surface expression detected as high degree of fluorescence (SKBR3 staining was not detectable). This means that 4T1 and human MDA-MB-231can be used as in vitro TNBC models for target study, while L929 and SKBR3 can be used as control cell lines. The cells in panels A & B are tested in same experiment, however C & D & E are testes in the other experiments. In Figures 3C, 3D, and 3E, both ICAM-1 and the nucleus are stained, while in Figures 3A and 3B, only ICAM-1 is stained. Collectively, these data indicate tht both 4T1 and MDA-MB-231 cancer cells expressed ICAM-1 at a higher degree than that of control cells, although 4T1 appeared to exhibit higher levels of ICAM-1 expression than that of human breast cacner MDA-MB-231.

3.3 Evaluation and selection of potential anti ICAM-1 ligands

3.3.1 Effects of NP on NP concentration dependent binding to MDA-MD-231 cells

We next investigated whether coating (or surface expression) of LFA1-P on NP particle surface could provide selective binding to cancer cells with over-expression of ICAM-1 receptor. We prepared NP particle with 0.4% indocyanine green (ICG), which exhibit near infrared fluorescence (λ_{ex}=789 (λ_{em}=819 nm emission). The binding of NP to cancer cell MDA-MB-231 was analyzed by the intensity of ICG fluorescence. As demonstrated in Fig. 4, ICG-NP is

associated to the cells at 4 ºC in a concentration (dose) dependent manner. The binding of NP reflected in the increase in fluorescence intensity with increasing concentrations of NP added in the cell incubation media. From 0 mM to 2 mM, the fluorescence intensity shows an approximately linear increase trend with increasing concentration. The fluorescence intensity increased slightly from 2 mM to 4 mM, but from 4 mM to 6 mM, the increasing fraction of fluorescence intensity per unit of lipid in the particles addition is dramatic. These data suggest that non-specific binding could be more prominent factor at higher NP concentrations. Therefore, we chose NP concentrations of 0~2 mM for further studies. This dose-dependent and apparent increase in off-target binding suggest a need define a dose range where targeted DcNP could provide beneficial therapeutic effects.

3.3.2 Effects of cyclic- LFA1-P, linear-LFA1-P peptide coated on NP on its ability to bind to ICAM-1 expressing cancer cells

To evaluate whether a cyclic peptide (which has been reported previously to lock in the binding domain structure of the LFA-1 binding to ICAM-1[27]) is required to provide recognition of ICAM-1 expressed on cancer cells, we have synthesized cyclic and linear version of LFA1-P LFA-1 peptide. The cyclic and linear LFA1-P peptides are coated on NP. With NP fluorescently labeled with ICG, we compared the ability of cyclic vs linear LFA1-P to provide cancer cell MDA-MB-231 localization at 4 ºC (to reduce phagocytic or internalization activity). 4 °C can minimize intracellular uptake and endocytosis of NP, and so the binding assay is performed under such conditions to allow evaluation of ligand-mediated NP binding. Under this condition, non-specific and intracellular uptake of NP is minimized. Data presented in Table 3 shows that at most NP concentrations, the ratio of fluorescence intensity of NP-linear-LFA1-P/NP and NP-cyclic- LFA1-P /NP was larger than 1, which indicates that ICAM-1 ligands can facilitate NP

binding to the MDA-MB-231 cancer cells. When the concentration is 0.5 mM, the cell binding of NP-linear-LFA1-P was largest, which was three times larger than NP and NP-cyclic- LFA1-P. However, the binding amount of NP-cyclic- LFA1-P was slightly higher than NP-linear-LFA1-P at a concentration of 1 mM. In addition, when concentration increased to 2 mM, non-specific binding took up the largest percentage of cell surface binding, which minimized the difference of NP binding between different drug formulation. Collectively, these data suggest that at low DcNP concentrations where non-specific DcNP uptake is low, linear peptides exhibit higher degree of peptide ligand mediated binding to cells, compared to that mediated by cyclic counterpart. Thus, for the rest of experiments, we used liner version of LFA1-P, instead of cycic peptide version. The (P) palmitoyl, which acts as a fatty acyl chair of hydrophobic domain of LFA1-P served as a stable anchor of LFA1-P of DcNP.

3.3.3 Effects of ICG fraction on ability to trace NP in vitro and in vivo

As the NP with 0.4% ICG has low fluorescence intensity and high variance, we next investigated the optimal density of ICG fluorescence label on DcNP on cell uptake in planning for *in vivo* DcNP targeting studies. As shown in Figure 5, increasing the percentage of ICG in the NP from 0.4% to 1% resulted in signal ~ 2.5 times higher after 37 °C incubation for 20 min. However, after 1h incubation at 4 °C, the intensity of NP (ICG 1%) is only ~2 times higher than NP (ICG 0.4%), which could be the result of experimental or analytical error. The result showed that 1% ICG in the DcNP formulation is sufficient and can consistently trace the fluorescence intensity of NP, so we used 1% ICG as a tagged for DcNP formulation for studies described below.

3.4 Effects of linear- LFA1-P, RGD and RGD-linear-LFA1-P peptide coated on NP on its ability to bind to ICAM-1 expressing cancer cells

With a refined ICG ratio, we next evaluated the targeting ability of linear-LFA1-P peptide, RGD peptide and their combination. Table 4 shows that the binding ability of NP-linear-LFA1-P was better than ligand free NP (ratio > 1). However, as for NP-RGD and NP-RGD-linear-LFA1-P in the graph, even if their binding amount is a little bit higher than NP, they did not show better binding capacity at 0.5 mM or 2 mM. This result (Table 4) is consistent with prior research that RGD has weak targeting effect to MDA-MB-231[28]. It might also be the reason why dual-ligand NPs did not show a better targeted effect. Therefore, based on all studies above, we choose linear-LFA1-P as the ligand for future study.

3.5 Effect of increasing *LFA1-P* peptide density on NP to enhance cell binding

The active targeting ability of NP may be related to the density of ligand. Thus, after selecting the most efficient ligand, we investigated the role of increasing LFA1-P mole percentage in DcNP on the binding ability of the DcNP to 4T1 cells. Figure 6 showed the relationship between the density of LFA1-P in NP and the intensity of the fluorescence signal. The fluorescent signal came from the amount of NP bound to the cell surface during the 1-hour incubation at 4 °C. Since the endocytosis is inhibited at 4 °C, the NP amount on the cell surface can represent the binding ability of the NP. In other words, each point in the figure represents the binding capacity of NP with 4T1 cells when LFA1-P density is same as the x axis. It could be seen from the figure that when the LFA1-P density is less than 2%, LFA1-P density and NP binding capacity were positively correlated. However, when the density of LFA1-P continued to increase, the binding capacity of NP began to decrease. When the LFA1-P density is increased to 5%, the binding capacity of NP is similar to that at 1% LFA1-P density. When LFA1-P density equals to 2%, NP binding ability reached to a highest point. Therefore, we assumed that the decreased binding ability when density equals to 5% may be caused by the changed structure of

NP induced by the incorporation of large amount of LFA1-P. In addition, as the fluorescence intensity of 2% LFA1-P has a high variation, it is difficult to conclude that 2% is significantly better than 1%. Regardless 1% or 2% LFA1-P could be used to provide ICAM-1 selective binding of DcNP to cancer cells.

3.6 Evaluation of Cytotoxicity of DcNP, DcNP-LFA1-P and GT free drugs combination in 4T1 cells

With a selected DcNP-LFA1-P formulation, we investigated efficacies of DcNP-LFA1-P and DcNP. Cytotoxicity of DcNP, DcNP-LFA1-P (1%), DcNP-LFA1-P (2%) and GT free drug combination were tested in 4T1 cell line. Table 5 summarized the IC_{50} of all the different formulations. The IC_{50} or cell mid-point of cell inhibitory drug concentration is a measure of drug potency against specific cells. Figure 7 (panel A) showed the IC_{50} of each drug for 4T1 breast cancer cells. We found that DcNP has the lowest IC_{50} value for gemcitabine 2.3 ng/mL, and DcNP-LFA1-P (2%) has a slightly higher IC_{50} value recorded at 3.9 ng/mL. However, the IC_{50} of DcNP-LFA1-P (1%), DcNP-LFA1-P (2%) and GT free drugs are in similar range indicating DcNP-LFA1-P did not provide apparent enhancement over that of DcNP for the same drug combination under static 5-day cell-culture conditions.

However, when DcNP is introduced in the body under dynamic conditions, the contact time of drugs either in DcNP or free form may be subjected to various flow and physiologic redistribution or wash out condition. Thus, we evaluated drug retention or residence time, cellular uptake rate based on short incubation and analysis after drug and DcNP cell washout. After 30 min coincubation with drugs, intracellular drug amount in the breast cancer cells was measured. In another experiment, the cells after brief drug exposure were allowed to grow for additional for 5 days to determine IC_{50}. Figure 7 (panel B) showed the IC_{50} of free drug

combination (0.060 μg/mL) is much higher than DcNP (1.038 μg/mL) or DcNP-LFA1-P (1.473 μg/mL). The higher IC_{50} of DcNP-LFA1-P than DcNP also indicate that LFA1-P incorporation did not appeared to improve rate of 4T1 cellular uptake or cellular residence time under these in vitro culture conditions. It is not known whether enhanced resident time and target binding of DcNP in vivo could provide additional benefit of LFA1-P coated on DcNP.

Collectively, the cell uptake study and cytotoxicity study suggested that LFA1-P can slightly enhance 4T1 cellular uptake of DcNP, and slightly increase the cytotoxicity of DcNP on 4T1 cells in 3 days incubation. But this enhancement did not appear to translate into in vitro e cellular uptake rate, drug maintenance time and cytotoxicity in 30 min incubation (washout study).

3.7 Effect of GT-DcNP targeted to ICAM-1 receptor on 4T1 breast cancer metastasize into the lung in mouse model.

3.7.1 Evaluation of time course 4T1 tumor metastasis in mice

In order to evaluate the treatment effect of DcNP, we perform a tumor progression time course to find a time window that could provide sufficient degrees neither too early nor too late in the progression where drug effect could not be measured. Therefore, we inoculated each animal with 200,000 cells, IV, and follow for 10 days. With 4T1 that express luciferase gene, we followed the increase in luciferase activity of bioluminescence in mice. As shown in Figure 8, the 4T1 cells grow can be visualized by IVIS imaging (Panel A) and quantified by tumor nodule counts (Panel B). It can be seen from Figure 8 (B) that in the first three days, tumors have not established in the lungs. On day 5, there were 7 nodules in the lungs, but the bioluminescence signal of tumors was not detected until the day 7. On day 12, the number of lung nodules had reached 46, and the fluorescence signal was very strong. When the lung tissue was analyzed under the microscope, the entire lung was fully occupied with tumors. For 4T1 metastatic breast

cancer mouse model, mice without treatment will lose 20% weight and need to be sacrificed after 14 days. Therefore, for therapeutic evaluation and DcNP drug targeting effects on lung metastases, we chose days 4 or 5 to initiate treatment in order to provide sufficient time for tumor with ICAM-1 to establish in mice and provide sufficient time for cancer treatment to see the tumor inhibition effect no later than day 14.

3.7.2 Effects of LFA1-P content on disbritutaion of ICG-labeled GT-DcNP (particles) in 4T1 metastatic breast cancer in mice

In vitro study described above has informed that a similar target ability of 1% and 2% LFA1-P, to determine the best LFA1-P density for *in vivo* study. Therefore, we first used 50/5 mg/kg (GT) based on the current clinical dose to compare the target ability of DcNP-LFA1-P (1%) and DcNP-LFA1-P (2%). Tumor imaging and drug concentration were both analyzed to have a better understanding of drug targeting ability. Mice were first inoculated with 4T1 cells and given a single IV dose of either DcNP, DcNP-LFA1-P (1 %) or DcNP-LFA1-P (2 %) formulations. 10 days interval after cell inoculation was selected as a drug treatment time, as this is the first day that tumor signal is sufficient to be detected by IVIS live imaging. The lung signal in Figure 9 (A) is obtained by IVIS imaging of 4T1 tumor bioluminescence, and the quantification lung luminescence intensity is shown in Figure 9 (B) and (C). From the intensity of the lung luminescence signal and the lung drug concentration, lung luminescence intensity of DcNP-LFA1-P (1%) is 2.6 times (live imaging) and 40 times (*ex vivo* imaging) higher than DcNP-LFA1-P (2%), it can be concluded that the binding ability of DcNP-LFA1-P (1%) is better than DcNP-LFA1-P (2%), so we selected 1% LFA1-P as LFA1-P density for *in vivo* study.

3.7.3 Effects of LFA1-P expressed on GT-DcNP on the lung gemcitabine and paclitaxel (GT) accumulations in 4T1 metastatic breast cancer mice

To determine the effects of enhanced drug exposure when presented in DcNP-LFA1-P dosage form, and compare with DcNP, GT CrEL drug combination (conventional formulation control), we used 50/5 mg/kg (GT) which is same as previous targeting study (3.7.3), treatment time was also keep consistent with previous study. Figure 10 (A) and (B) both showed that DcNP-LFA1-P has a better targeting ability and higher lung drug concentration than DcNP, 14 days after establishment of metastatic breast cancer in the lung. In addition, Figure 10 (A) showed a better drug accumulation of DcNP with 1% LFA1-P than 2% LFA1-P, Figure 10 (B) showed that compare to DcNP and DcNP-LFA1-P (1%), GT CrEL drug combination has the lowest lung drug concentration, GT-DcNP-LFA1-P significantly enhanced the G and T lung accumulation by 2.2 and 1.7 fold, respectively. The results indicate that drug combination nanoformulation targeted to ICAM-1 can an enhanced the both drugs to accumulate in cancer laden lung tissues, especially T, in lung tissues, and the incorporation of LFA1-P can further improve the accumulation of both drugs over that of DcNP.

3.7.4 Effect of LFA1-P on GT-DcNP to enhance inhibiting 4T1 metastatic nodules in the lungs.

To investigate whether the better targeting effect of DcNP-LFA1-P than DcNP translates to better efficacy, we evaluated the effect of DcNP-LFA1-P on inhibiting 4T1 lung metastasis. Mice were first inoculated with 4T1 cells and given a single IV dose of GT in CrEL, DcNP or DcNP-LFA1-P form. A low GT doses (5/0.5 mg/kg) was chosen to discern the targeting effect of DcNP-LFA1-P for DcNP, as this dose is previously shown to partially inhibit 4T1 lung tumor formation when given in DcNP dosage form[13]. Thus, we treated 4T1 mice at 3-hour post tumor inoculation with an intent to discern the targeting of LFA1-P in GT-DcNP, compared to that without (i.e., GT-DcNP alone) and evaluate the formation of lung metastasis nodules at day 14.

As shown in Figure 11, these lung nodules counting data indicate that a single dose of DcNP or DcNP-LFA1-P could significantly inhibit the establishment and growth of 4T1 metastatic cancer in the lungs than CrEL (free) drug combinations or Saline control. GT-DcNP-LFA1-P has a trend toward higher degree of tumor inhibition over that of GT-DcNP (by 11%). Due to the small sample size the data did not reach statistically significant ($p>0.05$). However, compared to free GT, the DcNP-LFA1-P exhibit highly significant treatment effects ($p=0.01$ DcNP-LFA1-P vs free GT), and a lower degree of significant for GT-DcNP ($p=0.04$ DcNP vs free GT).

These data indicates that the tumor inhibition of DcNP-LFA1-P to advancing cancer cells in blood for inhibiting the TNBC lung metastasis is not significantly better than GT-DcNP in a about 10-fold lower than clinically recommended (50/5 mg/kg GT) dose and with a sample size of 5 per group. The encouraging data collected with a single low dose and small number of animal study may need to be follow with a dose response study powered with a larger sample size. Given significantly higher lung drug accumulation with the targeted vs non-targeted GT-DcNP, further exploration is warranted to optimize the timing and multiple dosing schedule.

4 CONCLUSION

In conclusion, we have developed a strategy to target nanoparticles containing both gemcitabine and paclitaxel to metastatic breast cancer expressing ICAM-1 receptors. Using the ICAM-1 ligand, LFA1 mimic peptide and LFA1-P incorporated into DcNP, we were able to design a stable formulation of GT-DcNP-LFA1-P and evaluated its characteristics in cells and in a metastatic breast cancer model in mice. In vitro, LFA1-P enhanced NP binding with MDA-MB-231 and 4T1 cells. While in vitro cytotoxic potency in 4T1 cells appeared to be similar in a 5-day cytotoxicity assay, the interventional studies in 4T1 metastatic mouse models indicated

that adding LFA1-P to GT-DcNP significantly increased both gemcitabine (2.2 fold) and paclitaxel (1.7 fold) in the metastatic lung tissues. Early interventional studies with a low dose GT-DcNP in 4T1 models indicate that ICAM-1 targeted GT-DcNP may provide an additional degree of metastatic tumor nodule reduction by 14 days to a higher degree than that provided by an equivalent dose of free GT (also to a higher degree of significance when compared between targeted and non-targeted GT-DcNP to free drugs or untreated control groups).

Additional studies may be needed to explore the role of metastatic tumor establishment, providing a window of opportunity for the targeted DcNP to identify the time and dose optimal for applying targeted vs untargeted GT-DcNP for clinical translation. In addition, dose response studies may be needed to define the full range of efficacy and safety, and to define the therapeutic index. This targeted DcNP strategy may be useful to provide a higher safety and therapeutic response for other highly potent drugs in use or those in development for treating incurable metastatic breast cancers. It could also be used to develop longer lasting and more effective combination drug therapies for other diseases where drug-combination are needed to find a cure or effective treatment including chronic and acute lung infections.

Table 1. Composition of lipid excipients, palmitoylated LFA1-peptide, indocyanine green marker used in formulation of drug combination nanoparticles

	NP	NP-LFA1-P (0.5%)	NP-LFA1-P (1%)	NP-LFA1-P (2%)	NP-LFA1-P (5%)	
DSPC	89.19	87.84	85.14	89.64	88.74	mol %
DSPE-PEG_{2000}	9.91	9.76	9.46	9.96	9.86	mol %
Palm- LFA1-P	0	0.5	1	2	5	mol %
ICG	0.4	0.4	0.4	0.4	0.4	mol %
Total	100	100	100	100	100	mol %

Table 2. Size distribution and drug concentrations of NP with different size reduction methods.

Method & Instrument	Particle Size (diameter in nm for the two population)	Drug concentration (mg/mL)	
		T (2.1 mg/mL) *	G (6.6 mg/mL) *
Sonication (water bath)	82.8 (89.21%) 423.3 (10.79%)	1.96	6.98
Sonication (probe sonicator)	50.2 (81.1%) 153.5 (18.9%)	1.61	5.99
Extruder: LIPEX	55.8 (26.74%) 123.3 (73.26%)	0.15	2.39
Mini-extruder: Avanti	48.8 (31.27%) 115 (68.73%)	0.48	4.98

**DcNP containing T and G are prepared at 2.1 and 6.6 mg/mL respectively. The final concentrations determined after preparations based on HPLC as indicated in the Materials and Methods.*

Table 3. The ratio of the fluorescence intensity of NP (with ligand)/NP bound to 4T1 cells.

NP Concentration (mM)	Drug Formulations	
	NP-linear- LFA1-P	NP-cyclic- LFA1-P
0.5	4.31 ± 0.15	0.97 ± 6.21
1	16.60 ± 61.7	19.06 ± 61.8
2	1.47 ± 1.20	2.16 ± 0.73

Table 4. The ratio of the fluorescence intensity of NP (with ligand)/NP bound to 4T1 cells.

NP Concentration (mM)	Drug Formulation		
	NP-RGD	NP-linear-LFA1-P	NP-RGD-linear-LFA1-P
0.5	0.25 ± 0.08	1.15 ± 0.09	0.56 ± 0.19
1	1.13 ± 0.05	1.25 ± 0.06	1.50 ± 0.15
2	1.00 ± 0.02	1.20 ± 0.04	0.87 ± 0.03

Table 5. Effect of DcNP, DcNP-LFA1-P (1%), DcNP-LFA1-P (2%) and GT free drugs combination's ability to inhibit 4T1 cells.

	DcNP	DcNP-LFA1-P (1%)	DcNP-LFA1-P (2%)	GT free drugs combination
IC_{50} (ng/mL)	2.3	3.1	3.9	3.5
IC_{50} of washout study (μg/mL)	1.038	-	1.473	0.06

Figure 1. Photograph of an assembled LIPEX extruder.

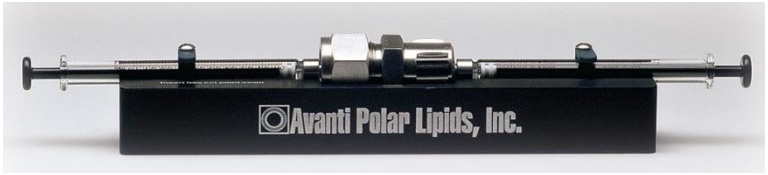

Figure 2. Photograph of an assembled Avanti mini-extruder.

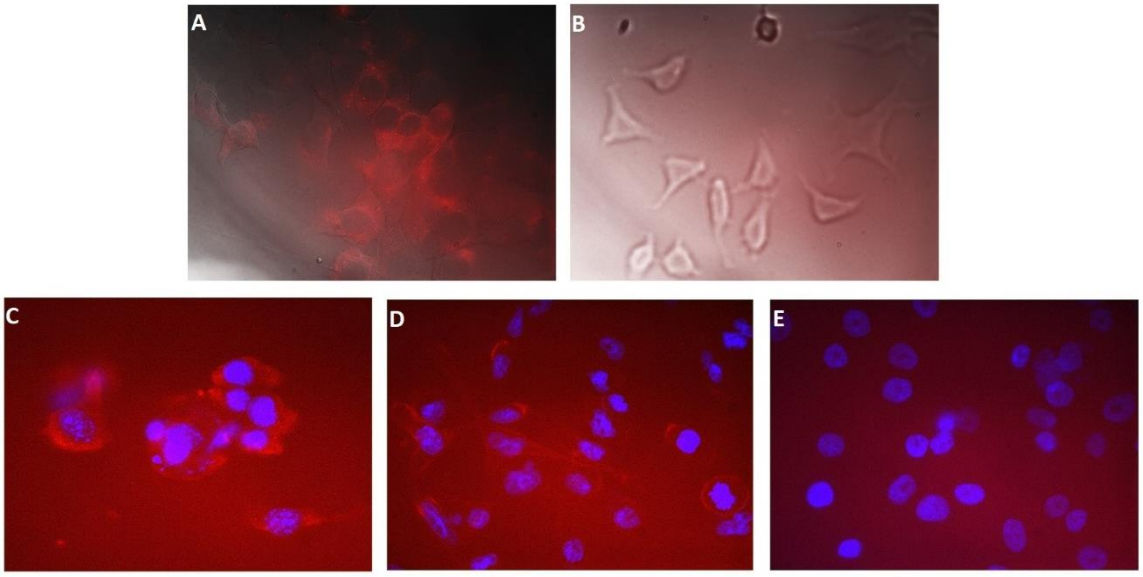

Figure 3. Immunofluorescent staining of ICAM-1 expression in 4T1 cells (A, C), L929 cells (B), MDA-MB-231 cells (D) and SKBR3 cells (E).

Cells were seeded into chamber slides (30,000 cells/well) and incubated overnight. Cells were fixed with PFA, quenched, and stained for ICAM-1 detection (red). In figure 3C, 3D and 3E, cell nuclei were stained with DAPI (blue). Each picture was chosen as representative of a triplicated experiment.

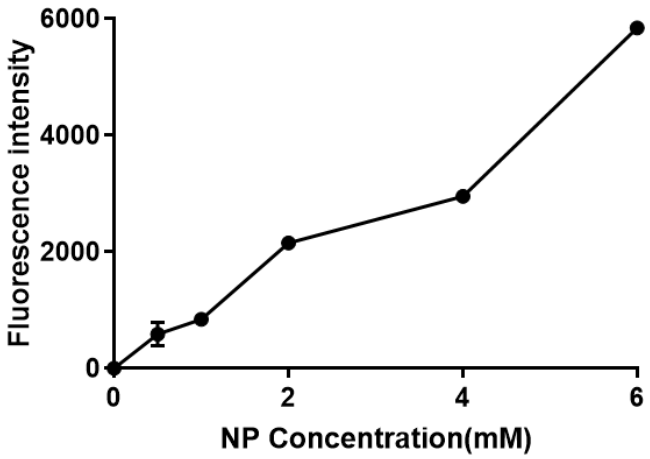

Figure 4. Dose response of fluorescence intensity of ICG-labeled NP bound to MDA-MB-231 cells.

A fixed concentration of NP-ICG was incubated with MDA-MB-231 cells in 6-well plate at 4 ºC for 1 hour. Fluorescence intensity was measured with a fluorometer as described in experimental procedures, the values in the figure are expressed as mean ± SD.

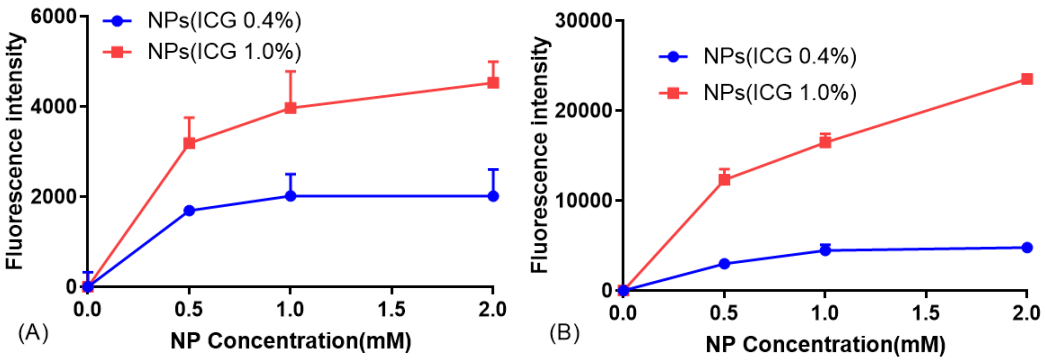

Figure 5. Optimization of ICG labeled incorporated into nanoparticles NP to provide higher ICG fluorescence yield.

Fluorescence intensity of NP with different ICG fraction (0.4 or 1 % of total nanoparticle's lipid excipients) were used for this experiment. The cell-associated IGC fluorescence intensity was determined with increasing dose of total NP concentrations added to MDA-MB-231 cells; after 1 hour incubation at 4 °C (panel A) and 20 min incubation at 37 °C (panel B) with. The values are expressed as mean ± SD of replicates.

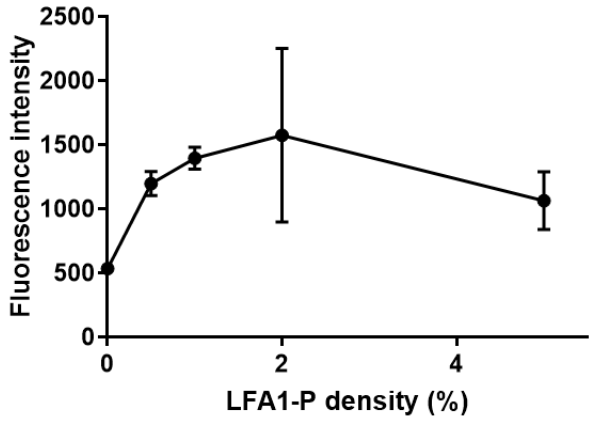

Figure 6. Effects of LFA1-P density on 4T1 cellular uptake of ICG-labeled nanoparticles

4T1 cells were seeded on a 12-well plate (300,000 cells/well) and incubated overnight. ICG-labeled NP with 0.5%, 1%, 2% and 5% LFA1-P of 0.5 mM (lipid concentration) were added into wells, and the plates were incubated at 4 °C (binding) for 1 hour or 37 °C (uptake) for 30 min. ICG Fluorescence intensity was measured in a micro-plate reader and the values are presented as mean ± SD of the replicates.

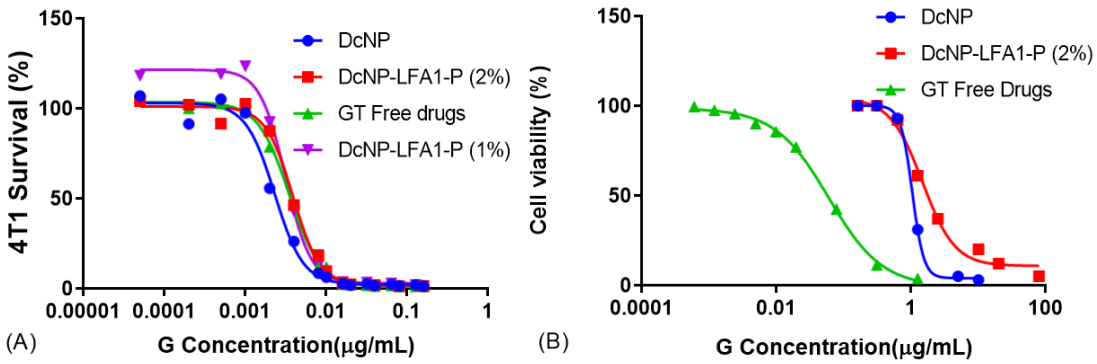

Figure 7. The effect of DcNP and DcNP-LFA1-P on growth of 4T1 cells.

Cell viability evaluated by the AlamarBlue assay (panel A) after 3 days incubation with DcNP, DcNP-LFA1-P and free drug combination (panel B) remove drugs from 96-well plate after 30 min incubation with 4T1 cells, and then incubate with new medium for 5 days. Concentrations are based on G, and the concentration of T is 1/10 of G. IC_{50} are listed in the Table 5.

(A) 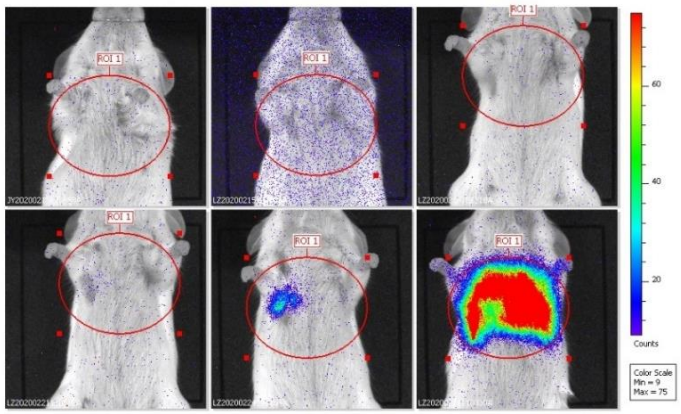

(B) 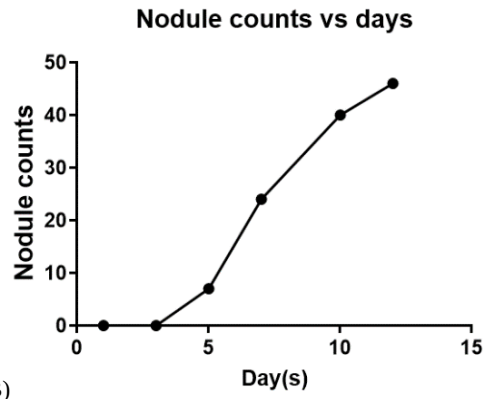

Figure 8. Time courses of 4T1 metastatic breast cancer spread into the lung and increasing number of cancer nodules in the lung.

Mice intravenously inoculated with breast cancer 4T1-luc (2, 000, 000 cells/mL). On day 1, 3, 5, 7, 10, 12, time dependent tumor spread and growth in the lung was monitored by 4T1-luciferase activity from each mouse detected. The data was presented as total bioluminescence intensity (panel A), and the lung tumor nodule counts (panel B).

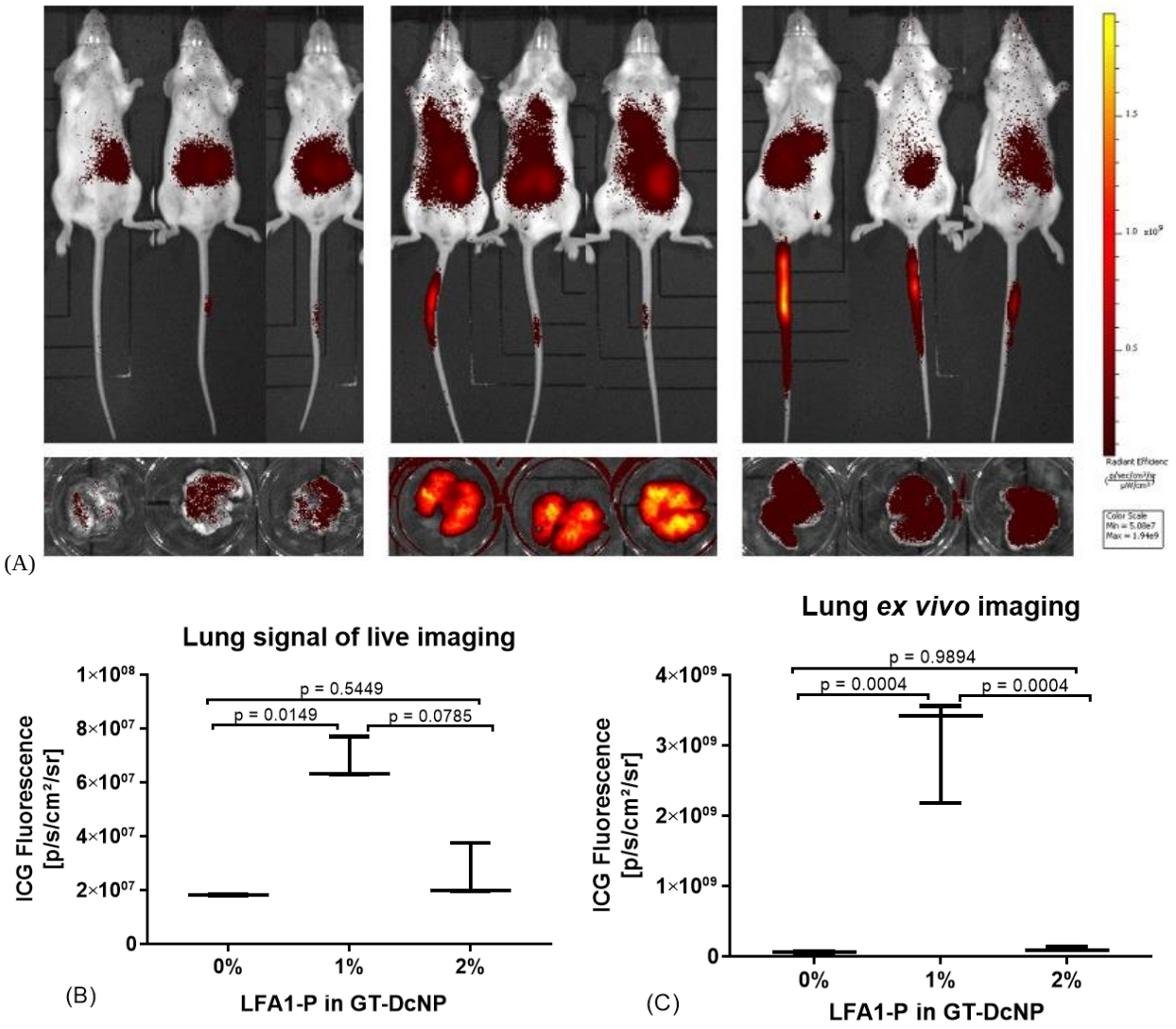

Figure 9. Effects of LFA1-P content on disbritutaion of ICG-labeled GT-DcNP (particles) targeting to 4T1 metastatic breast cancer in mice.

Mice inoculated with 4T1-luc breast cancer cells were administered with a single dose of ICG-labeled DcNP (containing 50/5 mg/kg GT, IV). These mice were imagined for ICG fluorescence and presented as whole-body image (Panel A), lung ICG intensity (Panel B), and the ICG intensity after remove of lung tissues. The effect of LFA1-P density on DcNP is determined with 0, 1 or 2 % of total lipid excipients concentration of ICG-GT-DcNP, as described in each panel. The data are expressed as mean ± SD (n=3). P values were obtained from two-tailed t-tests.

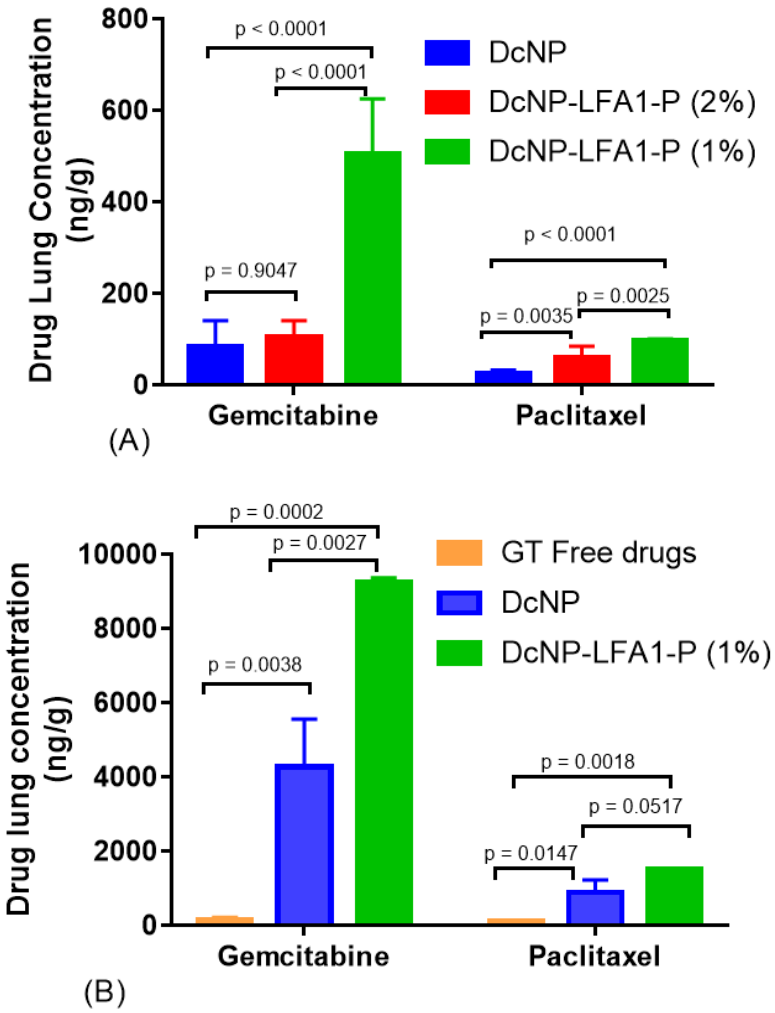

Figure 10. Effects of LFA1-P expressed on GT-DcNP on the lung gemcitabine and paclitaxel (GT) accumulations in 4T1 metastatic breast cancer mice.

Mice inoculated with 4T1-luc breast cancer cells were administered with a single dose of ICG-labeled DcNP (containing 50/5 mg/kg GT, IV). The total drug concentrations in lungs of these mice were determined. (panel A) DcNP and DcNP-LFA1-P with 1% or 2% of peptide. A follow-up experiment was done with GT in DcNP with or without of 1% LFA1-P, along with free GT in solution as a control (panel B). The data in (A) and (B) are displayed as mean ± SD (n=3). P values were derived with two-tailed t-tests.

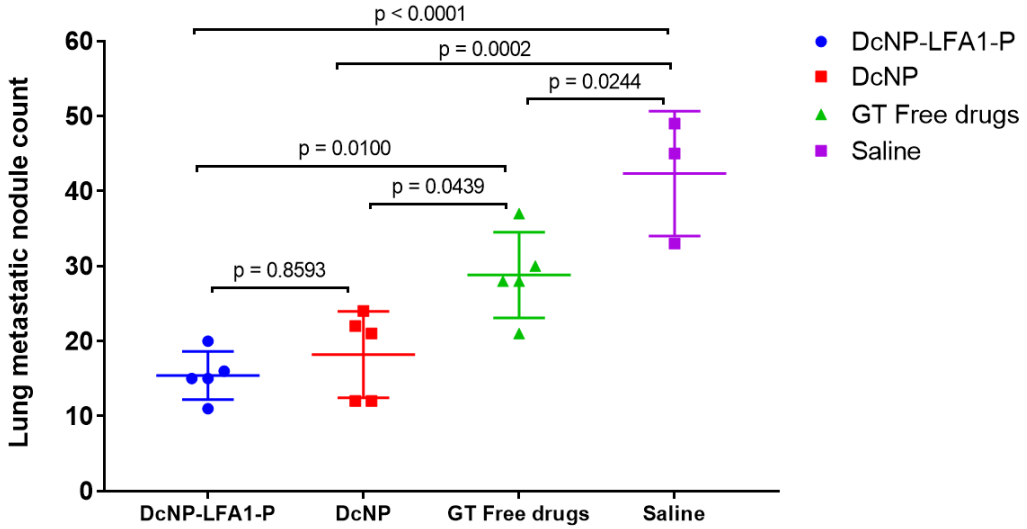

Figure 11. Effect of LFA1-P on GT-DcNP to enhance gemcitabine and paclitaxel to inhibit 4T1 metastatic breast cancer nodules in the lungs.

Mice inoculated with 4T1-luc via tail vein were administered with a 5/0.5 mg/kg GT in DcNP, DcNP-LFA1-P (1%) and GT CrEL (free) drug combination as a single IV dose (3 hours post inoculation). On day 14, the total 4T1 metastatic tumor nodules in the lung tissues for each treatment and group was calculated as mean ± SD. P values were obtained from 5 animals in each group base on two-tailed t-tests.

5 REFERENCES

1. Worldwide cancer data | World Cancer Research Fund. Accessed March 23, 2021. https://www.wcrf.org/dietandcancer/cancer-trends/worldwide-cancer-data

2. Arnedos M, Bihan C, Delaloge S, Andre F. Triple-negative breast cancer: Are we making headway at least? *Ther Adv Med Oncol*. 2012;4(4):195-210. doi:10.1177/1758834012444711

3. Gangi A, Chung A, Mirocha J, Liou DZ, Leong T, Giuliano AE. Breast-conserving therapy for triple-negative breast cancer. *JAMA Surg*. 2014;149(3):252-258. doi:10.1001/jamasurg.2013.3037

4. Telli ML, Sledge GW. The future of breast cancer systemic therapy: the next 10 years. *J Mol Med*. 2015;93(2):119-125. doi:10.1007/s00109-014-1238-y

5. Liyanage PY, Hettiarachchi SD, Zhou Y, et al. Nanoparticle-mediated targeted drug delivery for breast cancer treatment. Published online 2020. doi:10.1016/j.bbcan.2019.04.006.Nanoparticle-mediated

6. Kawada K, Taketo MM. Significance and mechanism of lymph node metastasis in cancer progression. *Cancer Res*. 2011;71(4):1214-1218. doi:10.1158/0008-5472.CAN-10-3277

7. Hirakawa S, Brown LF, Kodama S, Paavonen K, Alitalo K, Detmar M. VEGF-C-induced lymphangiogenesis in sentinel lymph nodes promotes tumor metastasis to distant sites. *Blood*. 2007;109(3):1010-1017. doi:10.1182/blood-2006-05-021758

8. Kraft JC, Mcconnachie LA, Koehn J, et al. Long-acting combination anti-HIV drug suspension enhances and sustains higher drug levels in lymph node cells than in blood cells and plasma. *Aids*. 2017;31(6):765-770. doi:10.1097/QAD.0000000000001405

9. Fletcher C V., Staskus K, Wietgrefe SW, et al. Persistent HIV-1 replication is associated with lower antiretroviral drug concentrations in lymphatic tissues. *Proc Natl Acad Sci U S A*. 2014;111(6):2307-2312. doi:10.1073/pnas.1318249111

10. Lorenzo-Redondo R, Fryer HR, Bedford T, Kim EY, Archer J KPS. Persistent HIV-1 replication maintains the tissue reservoir during therapy. *Physiol Behav*. 2017;176(3):139-148. doi:10.1038/nature16933.Persistent

11. Freeling JP, Ho RJY. Anti-HIV drug particles may overcome lymphatic drug insufficiency and associated HIV persistence. *Proc Natl Acad Sci U S A*. 2014;111(25):2512-2513. doi:10.1073/pnas.1406554111

12. Jennifer P. Freeling, Josefin Koehn, Cuiling Shu, Jianguo Sun and RJYH. Long-acting three-drug combination anti-HIV nanoparticles enhance drug exposure in primate plasma and cells within lymph nodes and blood. *AIDS*. 2014;176(1):2625–2627. doi:10.1097/QAD.0000000000000421.Long-acting

13. Mu Q, Yu J, Griffin JI, et al. Novel drug combination nanoparticles exhibit enhanced plasma exposure and dose-responsive effects on eliminating breast cancer lung metastasis. *PLoS One*. 2020;15(3):1-14. doi:10.1371/journal.pone.0228557

14. Yu J, Mu Q, Perazzolo S, et al. Novel Long-Acting Drug Combination Nanoparticles Composed of Gemcitabine and Paclitaxel Enhance Localization of Both Drugs in Metastatic Breast Cancer Nodules. *Pharm Res*. 2020;37(10). doi:10.1007/s11095-020-02888-8

15. Farokhzad OC, Cheng J, Teply BA, et al. Targeted nanoparticle-aptamer bioconjugates for cancer chemotherapy in vivo. *Proc Natl Acad Sci U S A*. 2006;103(16):6315-6320. doi:10.1073/pnas.0601755103

16. Werner ME, Copp J a, Karve S, et al. Folate-targeted Polymeric Nanoparticle Formulation of Docetaxel is an Effective Molecularly Targeted Radiosensitizer with Efficacy Dependent on the Timing of Radiotherapy. 2012;5(11):8990-8998. doi:10.1021/nn203165z.Folate-targeted

17. Guo P, Huang J, Wang L, et al. ICAM-1 as a molecular target for triple negative breast cancer. *Proc Natl Acad Sci U S A*. 2014;111(41):14710-14715. doi:10.1073/pnas.1408556111

18. Guo P, Yang J, Jia D, Moses MA, Auguste DT. ICAM-1-targeted, Lcn2 siRNA-encapsulating liposomes are potent anti-angiogenic agents for triple negative breast cancer. *Theranostics*. 2016;6(1):1-13. doi:10.7150/thno.12167

19. Sestak JO, Sullivan BP, Thati S, et al. Codelivery of antigen and an immune cell adhesion inhibitor is necessary for efficacy of soluble antigen arrays in experimental autoimmune encephalomyelitis. *Mol Ther - Methods Clin Dev*. 2014;1(January):14008. doi:10.1038/mtm.2014.8

20. Zhao H, Kiptoo P, Williams TD, Siahaan TJ, Topp EM. Immune response to controlled release of immunomodulating peptides in a murine experimental autoimmune encephalomyelitis (EAE) model. *J Control Release*. 2010;141(2):145-152. doi:10.1016/j.jconrel.2009.09.002

21. Yusuf-Makagiansar H, Anderson ME, Yakovleva T V., Murray JS, Siahaan TJ. Inhibition of LFA-1/ICAM-1 and VLA-4/VCAM-1 as a therapeutic approach to inflammation and autoimmune diseases. *Med Res Rev*. 2002;22(2):146-167. doi:10.1002/med.10001

22. Chittasupho C, Shannon L, Siahaan TJ, Vines CM, Berkland C. Nanoparticles targeting dendritic cell surface molecules effectively block T cell conjugation and shift response. *ACS Nano*. 2011;5(3):1693-1702. doi:10.1021/nn102159g

23. Abdollahi A, Griggs DW, Zieher H, et al. Inhibition of αvβ3 integrin survival signaling enhances antiangiogenic and antitumor effects of radiotherapy. *Clin Cancer Res*. 2005;11(17):6270-6279. doi:10.1158/1078-0432.CCR-04-1223

24. Lautenschlaeger T, Perry J, Peereboom D, et al. In vitro study of combined cilengitide and radiation treatment in breast cancer cell lines. *Radiat Oncol*. 2013;8(1):1. doi:10.1186/1748-717X-8-246

25. Oliveira-Ferrer L, Hauschild J, Fiedler W, et al. Cilengitide induces cellular detachment and apoptosis in endothelial and glioma cells mediated by inhibition of FAK/src/AKT pathway. *J Exp Clin Cancer Res*. 2008;27(1). doi:10.1186/1756-9966-27-86

26. Bretschi M, Merz M, Komljenovic D, Berger MR, Semmler W, Baüerle T. Cilengitide inhibits metastatic bone colonization in a nude rat model. *Oncol Rep*. 2011;26(4):843-851. doi:10.3892/or.2011.1373

27. Yusuf-Makagiansar H, Yakovleva T V., Tejo BA, et al. Sequence Recognition of α-LFA-1-derived Peptides by ICAM-1 Cell Receptors: Inhibitors of T-cell Adhesion. *Chem Biol Drug Des*. 2007;70(3):237-246. doi:10.1111/j.1747-0285.2007.00549.x

28. Bohn P, Modzelewski R, Rouvet J, et al. Biodistribution and imaging of [99mSUVmax]-HYNIC-RGD in MDA-MB-231 and NTERA-2 cancer cell xenografts. *Nucl Med Commun*. 2013;34(7):709-717. doi:10.1097/MNM.0b013e328361f552